Original Article

Evaluation of NanoDot Optically Stimulated Luminescence Dosimeter for Cone-shaped Small-field Dosimetry of Cyberknife Stereotactic Radiosurgery Unit: A Monte Carlo Simulation and Dosimetric Verification Study

Fadil Akyol, Neslihan Sarigul[1], Mete Yeginer, Yagiz Yedekci, Haluk Utku[1]

Department of Radiation Oncology, Faculty of Medicine, Hacettepe University, [1]Institute of Nuclear Science, Hacettepe University, Ankara, Turkey

Abstract

Aim: The aim of this study was to investigate the adequacy of nanoDot optically stimulated luminescence (OSL) dosimeter for small field dosimetry before its *in vivo* applications in CyberKnife SRS unit. **Materials and Methods:** A PTW 60018 SRS Diode, 60019 microDiamond, and Gafchromic EBT3 films were used along with a nanoDot carbon-doped aluminum oxide OSL dosimeter to collect and compare beam data. In addition, the EGSnrc/BEAMnrc code was employed to simulate 6-MV photon beams of CyberKnife SRS system. **Results:** All detectors showed good consistency with each other in output factor measurements for cone sizes of 15 mm or more. The differences were maintained within 3% for these cones. However, OSL output factors showed higher discrepancies compared to those of other detectors for smaller cones wherein the difference reached nearly 40% for cone size of 5 mm. Depending on the performance of OSL dosimeter in terms of output factors, percentage depth doses (PDDs) were only measured for cones equal to or larger than 15 mm. The differences in PDD measurements were within 5% for depths in the range of 5–200 mm. **Conclusion:** Its low reliable readings for cones smaller than 15 mm should be considered before its *in vivo* applications of Cyberknife system.

Keywords: CyberKnife SRS unit, Monte Carlo simulation, nanoDot optically stimulated luminescence dosimeter, small-field dosimetry

Received on: 21-09-2018 **Review completed on: 18-01-2019** **Accepted on: 18-01-2019**

Introduction

The developments in modern radiotherapy machines and treatment techniques have encouraged the use of nonuniform and small fields. While small fields provide more effective treatment options, new dosimetric challenges are encountered. The first codes of quality assurance (QA) for small-field dosimetry have been recently published for a systematic and universally incorporated approach to the dosimetry of small fields.[1] This report was prepared based on the study of Alfonso *et al*.[2] in which a new dosimetry formalism for small and nonstandard fields was proposed.

The challenges in small photon field dosimetry are stemmed from three factors: lateral electronic disequilibrium, source occlusion, and inappropriate detector dimensions.[2] Lateral charged particle disequilibrium exists when the maximum lateral range of secondary electrons are smaller than the field size. The dose measurement within the field becomes erroneous under disequilibrium since the balance of charged particles laterally scattered in and out of beam cannot be achieved. Moreover, due to the finite size of the source that is relatively large compared to small-field size, penumbrae over detector volume overlap and thus the relative central-axis dose reduces. "Inappropriate detector dimensions" mentioned in the third factor means that the perturbation of radiation field by detector increases as the field size decreases.

Access this article online

Quick Response Code:

Website: www.jmp.org.in

DOI: 10.4103/jmp.JMP_96_18

Address for correspondence: Prof. Fadil Akyol, Department of Radiation Oncology, Faculty of Medicine, Hacettepe University, Sihhiye, Ankara 06100, Turkey.
E-mail: hakyol@hacettepe.edu.tr

How to cite this article: Akyol F, Sarigul N, Yeginer M, Yedekci Y, Utku H. Evaluation of nanoDot optically stimulated luminescence dosimeter for cone-shaped small-field dosimetry of cyberknife stereotactic radiosurgery unit: A monte carlo simulation and dosimetric verification study. J Med Phys 2019;44:27-34.

All of three factors can affect detector response, and therefore, there are several studies focusing on the critical selection of detectors for small fields and their verification to improve the accuracy and precision of measured dose.[3-9] Total scatter factors in small fields were investigated by Francescon *et al*.[10] in which scatter factors measured with different detectors have shown a variability for the smallest collimators of Cyberknife system. Das *et al*.[4] also mentioned improving the accuracy of the small-field dosimetry was possible with small detectors which have minimum perturbation due to its presences and composition. Jang *et al*.[11] used a diode detector, ion chamber, and Gafchromic EBT3 film to measure beam data and compared them with the data obtained from other clinics with CyberKnife systems. Their results revealed that the beam data acquired using different detectors showed good consistency within ±3% for collimators larger than 20 mm. However, beam data for smaller cones have a discrepancy of 10% or more. Dieterich and Sherouse[12] investigated the variations in performances of commercially available diode dosimeters for quantitative small-field dosimetry, particularly by comparing the measurements of SRS cone factors. Morin *et al*.[13] compared plastic scintillation detectors with several commercial stereotactic dosimeters depending on the output factors and dose profiles using CyberKnife system. Their study also showed that current commercially available active detectors have limitations to perform accurate small-field dosimetry of the fields with a diameter <20 mm. As well as active ones, passive dosimeters have also been attractive for small field measurements. Bassinet *et al*.[14] observed an agreement (≤%2) between Gafchromic films and LiF microtubes for all output factors of Cyberknife and linear accelerators equipped with microMLCs and circular cones. They reported that these passive dosimeters do not require correction factors, and they can be used as reference dosimeters. Gel dosimeters, micro, and TLD dosimeters also have already been examined as passive dosimeters for small photon fields.[15,16]

Optically stimulated luminescence (OSL) dosimeters have gained popularity as passive dosimeters with applications for the verification of linac output calibration, brachytherapy source verification, QA of treatment plans, and clinical dose measurements.[17-21] Its linear dose response and high-dose sensitivity, which is 40–50 times greater than that of LiF TLD-100, make it an excellent material for dosimetry.[22,23] However, carbon-doped aluminum oxide (Al_2O_3:C) dosimeter also has a high effective atomic number of 11.28 causing the crystal over-response to X-rays in kV energy range.[22,23] Jursinic and Yahnke[24] examined built-up caps for OSL dosimeter and reported the influence of thickness and fabrication material of the built-up cap on field-size correction factors for *in vivo* dosimetry of conventional fields. Furthermore, Mrcela *et al*.[25] investigated a commercial InLight OSL system for *in vivo* applications and they noted that their system represents a valid alternative to other *in vivo* dosimetry systems.

The aim of the current study is to evaluate the performance of the nanoDot OSL dosimeter in small field dosimetry before its *in vivo* applications in CyberKnife SRS unit. Gafchromic films, microDiamond, and SRS diode detectors were used to compare its performance in the measurements of output factors and depth dose profiles. The EGSnrc/BEAMnrc code was also used to simulate 6 MV photon beams of CyberKnife system. The attractiveness of nanoDot OSL originates from its rapid and well-controlled optical readout and the possibility of re-estimation of the absorbed dose along with its high sensitivity of Al_2O_3:C.[22-28]

Materials and Methods

NanoDot optically stimulated luminescence dosimeter

OSL dosimeters used in this study were NanoDots™ (Landauer, Inc., Glenwood, IL, USA) which consist of Al_2O_3:C sensitive material placed in a plastic casing. The sensitive volume – a disk of diameter 5 mm and thickness 0.2 mm – is encased in a 0.05-mm thick polyester binding foil. The overall thickness of the disk is 0.3 mm. The height of the air gap both above and below the active volume is 0.49 mm. The outer black light-tight plastic casing of 10 mm × 10 mm × 2 mm has a mass density of 1.03 g/cm^3 and the thickness of plastic leave that covers both sides of the OSL disk is 0.36 mm.[17,29-33] Since Monte Carlo (MC) simulation of the dose distribution for nanoDot OSL dosimeter is essential for our study, the given physical parameters were used in our modeling.

To perform our experiment, OSL dosimeter was wrapped with paraffin material to eliminate any gap that may exist between the phantom and the dosimeter and subsequently placed between slabs of a water-equivalent phantom [Figure 1]. First, OSL dosimeters were calibrated using 6 MV photon beam with a solid water phantom of dimensions of 30 mm × 30 mm × 30 cm and a standard setup of depth (d_{max}) 1.5 cm, SSD 100 cm, and field size of 10 cm × 10 cm.

Each OSL measurement was repeated three times with separate OSL dosimeters to obtain the mean dose value. The

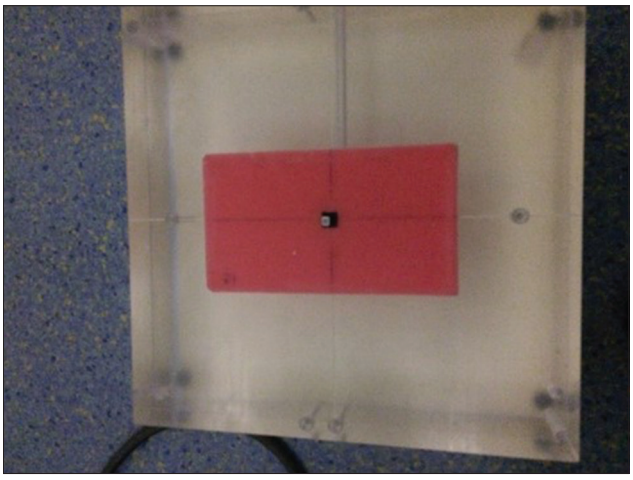

Figure 1: Measurement setup of nanoDot optically stimulated luminescence dosimeter. The chip is wrapped with paraffin material and placed between slabs of solid water phantom

measurement error was calculated as the standard deviation of three readings. The readings of OSL dosimeters were obtained using a microStar reader (Landauer, Inc., Glenwood, IL, USA). The postirradiation reading was taken at least 30 min after irradiation for a stable number of counts.[17,34] Bleaching was performed using a LED bulb emitting 1300 lm of white color (Storia Luca, China). After an overnight bleaching for 18–24 h, the chip readout was observed to be <200 counts.[34]

Gafchromic EBT3 film

The film used in this study was Gafchromic EBT3 (Ashland Specialty Ingredients, Bridgewater, NJ). The polyester used in EBT3 has a special surface treatment with microscopic silica particles. Its detailed specifications can be found elsewhere.[35]

These films were cut into pieces of 5 cm × 6 cm before irradiation. This size covers an area to limit the statistical uncertainties during irradiation and analysis.[36,37] Gafchromic film dosimetry is not a real-time technique and requires much more time compared to active ones. Each film was scanned three times before irradiation to determine the mean background value. The films were stored before and after irradiations in opaque envelopes inside a dark-lined cardboard box to prevent exposure to light. The films were scanned 24 h after irradiations using Epson Expression 10,000XL scanner to allow postirradiation color changes. Every scan was repeated three times with the transmission mode (positive film mode), 48-bit RGB (16 bits per channel color), and resolution of 75 dpi without any image correction.

We followed the recommendations of Yu *et al*. for the scanning process.[38] The results obtained from 1 cm outer edge of the scanned film was excluded to minimize its effect on scanner results. The average pixel values lying within a circle of appropriate diameter at the corresponding radiation field center were taken, and they were used for the calculation of optical density (OD). The uncertainty in calculated OD was determined using the standard deviation of average pixel value obtained from the region of interest.

PTW 60018 diode SRS and PTW 60019 microDiamond

The detectors used in this study were manufactured by Physikalisch-Technische Werkstatten (PTW, Freiburg, Germany). According to their user manuals, PTW 60018 diode has a sensitive volume of 0.3 mm^3 with a circular area of 1 mm^2 and thickness of 250 μm. The radius of sensitive volume is 0.6 mm. The detector material is p-type silicon, and the area density is 0.14 g/cm^2. Furthermore, PTW 60019 microDiamond detector is a synthetic single-crystal diamond detector and has a very small sensitive volume of 0.004 mm ≥ with a circular radius of 1.1 mm and thickness of 1 μm.

Irradiation procedure and experimental measurement

The measurements of PTW 60019 and PTW 60018 detectors were performed in a water phantom (MP3 Water Scanning System, PTW) whereas NanoDots and Gafchromic films were sandwiched between plastic water-equivalent slabs with the dimensions of 30 cm × 30 cm (Gamme × 457, Gammex, Middleton, USA). The output measurements were performed at a depth of 15 mm, and percentage depth doses (PDDs) were obtained with an increment of 5 mm. All measurements were obtained at source to surface distance (SSD) 80 cm for depth dose curves and at 80 cm SDD for output factors. The dose measurements at each point were repeated three times, and 100 MU was delivered per measurement.

The output factors were evaluated using the following equation:

$$\Omega^{f_{clin}f_{msr}}_{Q_{clin}Q_{msr}} = \frac{M^{f_{clin}}_{Q_{clin}}}{M^{f_{msr}}_{Q_{msr}}} . k^{f_{clin},f_{msr}}_{Q_{clin},Q_{msr}} = s_{c,p} . k^{f_{clin},f_{msr}}_{Q_{clin},Q_{msr}} \quad (1)$$

where $M^{f_{clin}}_{Q_{clin}}$ and $M^{f_{msr}}_{Q_{msr}}$ refer to detector readings per MU in the fields, f_{clin} and f_{msr}, respectively; f and Q represent collimator size and beam quality, respectively; *clin* and *msr* represent the clinical and machine-specific reference field sizes; $k^{f_{clin},f_{msr}}_{Q_{clin},Q_{msr}}$ is the correction factor required to determine the dose deposited to water between f_{clin} and f_{msr} owing to the presence of detector in water; $\Omega^{f_{clin}f_{msr}}_{Q_{clin}Q_{msr}}$ is the output factor or total scatter factor.

In our study, the depth dose measurements were not obtained for the cone sizes of 5 mm, 7.5 mm, and 10 mm, since the discrepancy between OSL readings and other dosimeter results was determined to be higher than 3% for the cone sizes smaller than 15 mm. Therefore, the correction factors for OSL dosimeter were not required for acquired OSL readings.

Monte Carlo simulations

The output factors and depth dose profiles were calculated using EGSnrc/BEAMnrc MC code[39,40] in conjunction with DOSXYZnrc code. Phase space files for each cone size of 5, 7.5, 10, 12.5, 15, 20, 30, 40, and 60 mm were generated using a modeled treatment head of CyberKnife SRS system.[28] The incident electron mean energy and full width at half maximum of the electron radial intensity distribution were 6.7 MeV and 3.2 mm, respectively. The global electron and photon cut-off energies for particle transport were set to 700 keV (total energy) and 10 keV, respectively.

The phase space data were used as a source for DOSXYZnrc. MC calculations were performed for two main models. In the first model, a water phantom with dimensions of 30 cm × 30 cm × 30 cm was modeled for MC simulation using different voxel sizes between 0.5 and 5 mm to obtain the dose values for the volume of interest in water. The calculated values for water were used as a reference. The second model included an OSL dosimeter placed between poly (methyl methacrylate) phantom slabs as shown in Figure 1. The voxel size was chosen as 0.1 mm × 0.1 mm × 0.04 mm to fit the dimensions of OSL dosimeters properly. The sensitive material contains a very small amount (0.01%–0.5%) of carbon doping,[33,41] which was not considered in the simulations. The plastic casing of dosimeter was geometrically complex and nearly water equivalent (1.03 g/cm^3); thus, it was neglected in the model.

The OSL nanoDot material compositions were fed into the PEGS4 library. The cutoff energy thresholds for electron and photon were set to 700 and 10 keV respectively. The fractional energy loss per electron step was set to 2.5% (ESTEPE = 0.025). NSplit was chosen to be 30.[42] Using these specifications, histories between 3×10^7 and 6×10^8 were required to achieve an uncertainty of <1%.

The output measurement ratio defined in the following equation can be computed directly using MC simulation:

$$\Omega_{Q_{clin} Q_{msr}}^{f_{clin} f_{msr}} = \frac{D_{w,Q_{clin}}^{f_{clin}}}{D_{w,Q_{msr}}^{f_{msr}}} = \frac{D_{MC,w,Q_{clin}}^{f_{clin}}}{D_{MC,w,Q_{msr}}^{f_{msr}}} \cdot \frac{D_{MC,mon,Q_{msr}}^{f_{msr}}}{D_{MC,mon,Q_{clin}}^{f_{clin}}} \quad (2)$$

where $D_{MC,w,Q_{clin}}^{f_{clin}}$ and $D_{MC,w,Q_{msr}}^{f_{msr}}$ represent the doses deposited in water per simulated history with the clinical fields (f_{clin}) and machine-specific field (f_{msr}), respectively; $D_{MC,mon,Q_{clin}}^{f_{clin}}$ and $D_{MC,mon,Q_{msr}}^{f_{msr}}$ represent the total dose per initial history scored within the monitor chamber with MC simulation; Q_{msr} and Q_{clin} represent the beam quality of machine-specific field f_{msr} and the clinical field f_{clin}, respectively.

Results

Output factor

Measurements were carried out to compare the output factors of nanoDot OSL dosimeter with those of PTW 60018 and PTW 60019 detectors and Gafchromic EBT3 films for the nine collimators of 5, 7.5, 10, 12.5, 15, 20, 30, 40, and 60 mm. The MC output factors under reference conditions of water were also included for comparison. The equations required to calculate the output factors were given by equations (1) and (2).[2] The comparison between the measured output factors of given detectors and the calculated output factors of MC simulation with respect to the collimator sizes is illustrated in Figure 2. The relative uncertainties of the results were calculated with respect to the average values of repeated measurements. While the relative uncertainties of PTW 60018, PTW 60019, EBT3 film, and reference MC output factors were <1% for all cone sizes, the relative uncertainties of nanoDot dosimeters were 1.7%, 1%, and 1.4% for 5, 7.5, and 10 mm, respectively. Figure 2 illustrates the deviation of nanoDot OSL outputs compared to the rest of group. It was considered that the deviation for smaller collimator sizes indicated a deviation from accuracy. However, the observed deviations should not be attributed to inaccurate response of dosimeter material (Al_2O_3) but to its relatively large diameter of 5 mm. As the collimator size became closer to the size of dosimeter, larger perturbations in dose distributions were inevitable.

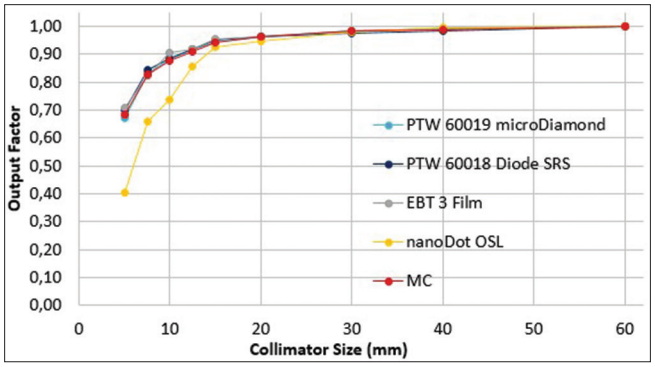

Figure 2: Measured output factors, $s_{c,p}$, of the detectors used in this study and Monte Carlo output factors under reference conditions. The output factor values were normalized with the reading of largest cone of 60 mm for each dosimeter

Table 1 lists the deviations of OSL output factors from those of other three dosimeters and reference MC simulation. For the larger cone sizes between 30 and 60 mm, the output factors of OSL were observed to be within 1% of the output factors of EBT3 film, two PTW detectors, and reference MC simulation. As the cone size reduced, the difference between the output factors of OSL and EBT3 film became even worse for the 5-mm cone by reaching 43% (e.g., it reached 3% for the 15-mm cone).

We observed that the results of reference MC simulations were consistent with the measured output factors of the OSL dosimeters, except for the small cone sizes of 15 mm and less as clearly seen in Table 1 (e.g., the deviation rose sharply to 41.3% for the cone size of 5 mm). The large discrepancies in the output readings of the nanoDot OSL dosimetry for smaller beam sizes in spite of high sensitivity and accuracy of Al_2O_3:C material showed that OSL dosimeters should be downsized as demonstrated in a previous study.[17] The output results of PTW 60019 and PTW 60018 compared to reference MC calculations were within approximately 1% or less for the cone sizes of 10 mm and more. However, the difference increased to 1.9% and 2.2% for the cone size of 5 mm for PTW 60019 and PTW 60018, respectively. The deviation

Table 1: Relative differences of the output factors of PTW 60019, PTW 60018, EBT3 film, and reference Monte Carlo from nanoDot optically stimulated luminescence dosimeter

Cone sizes (mm)	PTW 60019 (%)	PTW 60018 (%)	EBT3 (%)	MC (%)
5	−39.6	−41.95	−42.69	−40.78
7.5	−21.03	−22.08	−20.31	−20.4
10	−16.02	−16.57	−18.36	−15.8
12.5	−6.61	−6.77	−6.75	−5.83
15	−1.65	−2.7	−2.94	−1.93
20	−1.96	−1.65	−1.84	−1.74
30	−0.11	0.52	−0.05	−0.11
40	0.31	1.02	0.43	0.53
60	-	-	-	-

MC: Monte Carlo, PTW: Physikalisch-Technische Werkstaetten, OSL: Optically stimulated luminescence

from reference MC values remained approximately 1% until cone size of 12.5 mm but reached 3% for smaller cone sizes for Gafchromic EBT3 film.

Depth dose profile

Depth dose profile measurements and the corresponding MC simulations were performed for the cone sizes between 15 and 60 mm since the discrepancies between the readings of OSL and those of other dosimeters exceeded 3% for the cones smaller than 15 mm. The PDD results are shown in Figure 3. As shown in Figure 3, MC refers to the depth dose values of the modeled water phantom whereas MC_OSL refers to the PDD values calculated using the modeled nanoDot OSL dosimeter at different depths in a water phantom.

At surface region, large discrepancies among PDD values were observed. For instance, the difference reached 45% at 1 mm depth for the cone size of 20 mm. From 5 mm depth, the discrepancy decreased and remained within 5%. The differences between PDD values acquired using nanoDot OSL dosimetry and the other dosimetric systems are shown in Figure 4. The data showed higher deviations with measurement depth for all four-cone sizes. The deviations were generally maintained within 2% until the depth of 100 mm, particularly

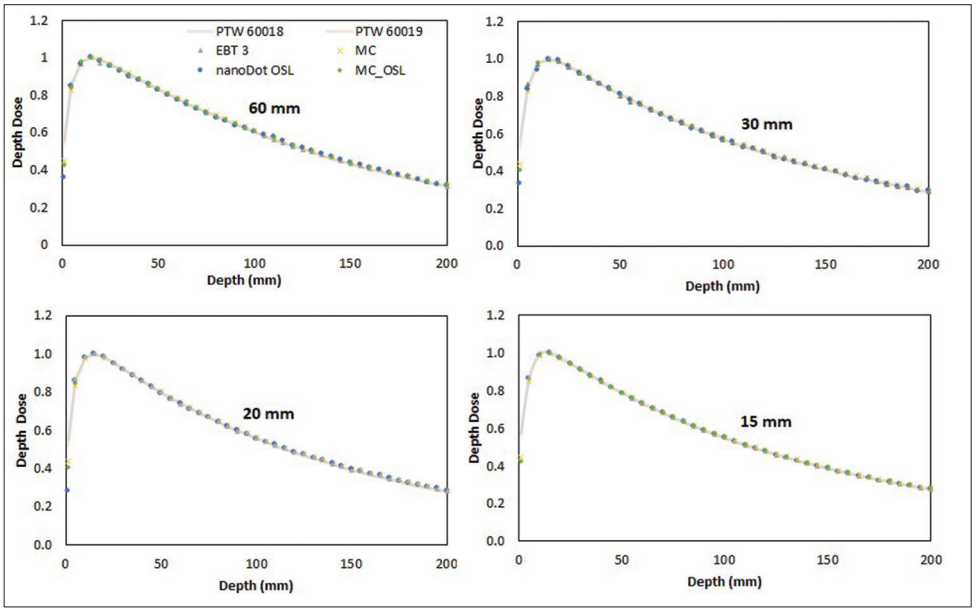

Figure 3: Comparison of measured and calculated central axis depth-dose curves for cone sizes of 60 mm, 30 mm, 20 mm, and 15 mm

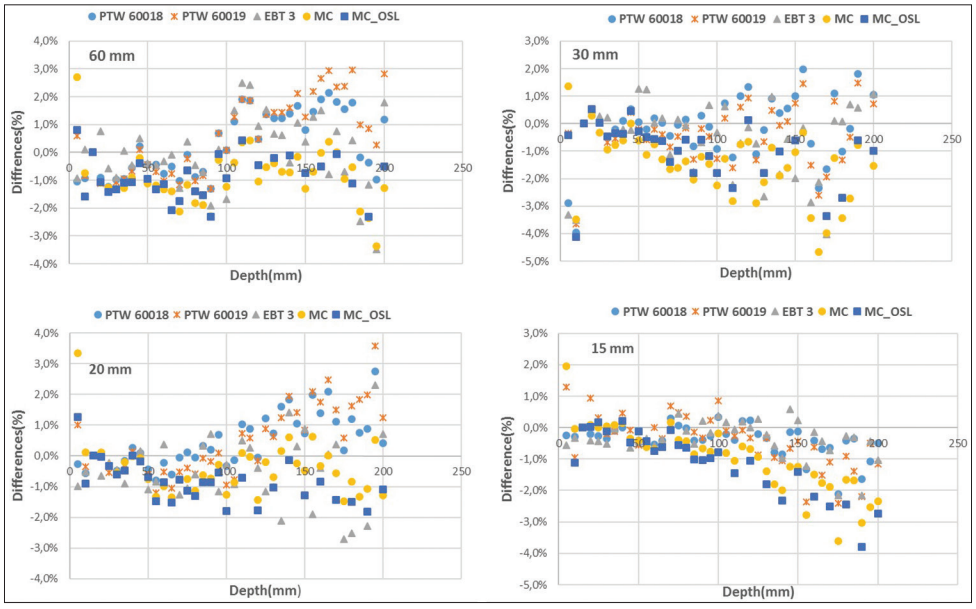

Figure 4: Differences between percentage depth dose readings of the nanoDot optically stimulated luminescence and those of PTW 60018, PTW 60019, EBT3 film, Monte Carlo, and Monte Carlo_optically stimulated luminescence for the cone sizes of 60 mm, 30 mm, 20 mm, and 15 mm

after the depth of dose maximum (15 mm). After this depth, the deviations became larger, i.e., within 5%.

Table 2 presents the PDD values at 10 cm depth for active and passive detectors used in this study. The columns under "%diff" in the table show the relative difference with respect to the detector in question. The OSL readings at 10 cm depth were observed to be consistent with the other readings. The deviations from both MC simulations were within 2% whereas the other dosimetry readings were closer to the OSL readings and their absolute "%diff" values were <1%.

Discussion

Routine quality assurance of a CyberKnife SRS unit must be performed accurately and precisely to deliver treatment to a patient as prescribed. A feasibility study designed for determining a proper dosimeter for the CyberKnife QA that may reduce the uncertainty induced by the cone-shaped small fields is critical for accomplishing accurate stereotactic treatment delivery with acceptable quality. Our study was designed for analyzing the performance of nanoDot OSL dosimeter for the measurement of the output factors and PDDs of small fields shaped by the fixed cones of CyberKnife unit.

Despite the advantageous features of an OSL dosimeter for standard radiotherapy fields, small fields provide challenging issues that reveal its limitations. The bell-shaped forms of filter-free small fields reveal the need for a small sensitive volume of the dosimeter more clearly, while reducing the cone size. In the measurements of relative output factors, the discrepancies between OSL readings and other three dosimeter measurements and MC calculation results were <1% for the cone sizes larger than or equal to 30 mm. The differences were observed to be in the range of 1%–3% for the cones between 30 and 15 mm. Moreover, the discrepancies exceeded 5% for the cone size of 12.5 mm and reached approximately 40% for the cone size of 5 mm. Chalkley and Heyes[43] similarly measured the relative output factors of CyberKnife fixed cones using six detectors including PTW 31010 Semiflex, PTW 60018 diode SRS, and PTW 60019 microDiamond. PTW 31010 showed consistent readings with OSL data as similar to our study since its diameter (5.5 mm) is comparable to that of the nanoDot OSL dosimeter. The reported output readings of the Semiflex were consistent with the diode SRS and microDiamond until the cone size of 20 mm. As the cone size became smaller, the differences increased in our study. The relative output factor values of Semiflex for cone sizes of 7.5 mm and 5 mm were observed to be approximately 67% and 38%, respectively. These values are close to our nanoDot OSL readings of 66% and 41%, respectively. However, diode SRS and microDiamond with diameters smaller than 2.2 mm were consistent with MC simulations even for the smallest cone sizes in our study. EBT3 film with high two-dimensional (2D) resolution could also provide consistent results with the two dosimeters for the challenging small field sizes.

The PDD measurements were obtained only for the cone sizes larger than or equal to 15 mm since the discrepancy between the readings of OSL and those of other dosimeters exceeded 3% for smaller cones. The performance of nanoDot OSL dosimeter in PDD measurement was observed to be consistent with other dosimeter readings in the region of transient charged particle equilibrium. However, in the build-up region, the readings of dosimeters were inconsistent especially at near-surface depths.

In the PDD measurements, the high number of measurement points revealed high workload required to obtain a PDD curve using the nanoDot OSL dosimeter. Changing the OSL dosimeter for each point and renewing the measurement setup increased the total QA time and workload compared with online data acquisition process using diode SRS and microDiamond detectors. Furthermore, the two dosimeters will also require the physicist to go into the bunker and arrange the slab phantom depth for each measurement point if PDD curve is acquired using solid phantoms. If a water phantom is chosen, the setup time of water phantom should also be taken into consideration.

The output factor measurements obtained for cone sizes smaller than 15 mm demonstrate that nanoDot OSL dosimeter should be modified to be suitable for the routine QA of smallest cones in CyberKnife system. As stated before, the first idea in this direction is to downsize the diameter of 5 mm of nanoDot OSL chips. In a study investigating detector correction factors for small-field applications,[44] Al_2O_3:C dosimetry with smaller dimensions of 0.5 mm × 0.5 mm × 2 mm was also recommended for commissioning owing to its relatively small correction factors. Alternatively, recently developed OSL films with high 2D resolution can be evaluated for the relative dose measurements of CyberKnife small fields.

Table 2: Measured and calculated percentage depth dose values at the depth of 10 cm and relative differences from optically stimulated luminescence readings

Cone size (mm)	PTW 60018		PTW 60019		MC		MC_OSL		nanoDot OSL	EBT 3	
	PDD	%diff	PDD	%diff	PDD	%diff	PDD	%diff		PDD	%diff
60	60.2	-0.2	60.2	-0.2	61.3	1.6	61.0	1.1	60.3	60.8	0.8
30	57.1	0.5	57.3	0.9	57.9	1.9	57.6	1.4	56.8	56.8	0.0
20	55.7	0.3	56.0	0.9	56.2	1.2	56.5	1.8	55.5	55.6	0.2
15	55.0	-0.4	54.7	-0.9	55.3	0.2	55.6	0.8	55.2	54.9	-0.5

*MC: Monte Carlo simulation, MC_OSL: Monte Carlo simulation of OSL, %diff: Relative difference from OSL readings, PDD: Percentage depth dose, PTW: Physikalisch-Technische Werkstaetten, OSL: Optically stimulated luminescence

A new 2D-dosimetric system was recently characterized for standard photon fields and demonstrated promising results in high-gradient dose regions.[45]

Conclusions

The readings of the nanoDot OSL dosimetry were consistent with the measurements of microDiamond, SRS diode detector, and Gafchromic films for cones larger than 15 mm while high discrepancies were found for the smaller cones. In spite of its linear dose response, high dose sensitivity and well-controlled read-out system, its low reliable behavior for the cones smaller than 15 mm should be taken into account before its *in vivo* applications of Cyberknife SRS unit.

Acknowledgment

The authors are grateful to Professor Erdem Karabulut, Hacettepe University Department of Biostatistics for his valuable evaluation of our data and Professor Fujio Araki, Kumamoto University, Japan for his kind help in the MC simulation section of the study. The first two authors contributed equally to this article.

Financial support and sponsorship

This study was supported by The Scientific and Technological Research Council of Turkey with grant number 114S753.

Conflicts of interest

There are no conflicts of interest.

References

1. Palmans H, Andreo P, Huq MS, Seuntjens J, Christaki K. Dosimetry of Small Static Fields Used in External Beam Radiotherapy: An IAEA-AAPM International Code of Practice for Reference and Relative Dose Determination. Technical Report Series No. 483. Vienna: International Atomi Energy Agency; 2017.
2. Alfonso R, Andreo P, Capote R, Huq MS, Kilby W, Kjäll P, *et al.* A new formalism for reference dosimetry of small and nonstandard fields. Med Phys 2008;35:5179-86.
3. Biasi G, Petasecca M, Guatelli S, Martin EA, Grogan G, Hug B, *et al.* CyberKnife® fixed cone and iris™ defined small radiation fields: Assessment with a high-resolution solid-state detector array. J Appl Clin Med Phys 2018;19:547-57.
4. Das IJ, Ding GX, Ahnesjö A. Small fields: Nonequilibrium radiation dosimetry. Med Phys 2008;35:206-15.
5. Veselsky T, Novotny J, Jr., Pastykova V, Koniarova I. Determination of small field synthetic single-crystal diamond detector correction factors for CyberKnife, Leksell Gamma Knife Perfexion and linear accelerator. Phys Med 2017;44:66-71.
6. Masi L, Russo S, Francescon P, Doro R, Frassanito MC, Fumagalli ML, *et al.* CyberKnife beam output factor measurements: A multi-site and multi-detector study. Phys Med 2016;32:1637-43.
7. Wilcox EE, Daskalov GM. Evaluation of GAFCHROMIC EBT film for cyberknife dosimetry. Med Phys 2007;34:1967-74.
8. Huet C, Dagois S, Derreumaux S, Trompier F, Chenaf C, Robbes I. Characterization and optimization of EBT2 radiochromic films dosimetry system for precise measurements of output factors in small fields used in radiotherapy. Radiat Meas 2012;47:40-9.
9. Fukata K, Sugimoto S, Kurokawa C, Saito A, Inoue T, Sasai K, *et al.* Output factor determination based on monte carlo simulation for small cone field in 10-MV photon beam. Radiol Phys Technol 2018;11:192-201.
10. Francescon P, Kilby W, Noll JM, Masi L, Satariano N, Russo S, *et al.* Monte carlo simulated corrections for beam commissioning measurements with circular and MLC shaped fields on the cyberknife M6 system: A study including diode, microchamber, point scintillator, and synthetic microdiamond detectors. Phys Med Biol 2017;62:1076-95.
11. Jang J, Kang YN, Shin HJ, Seo JH, Kim MC, Lee DJ, *et al*. Measurement of beam data for small radiosurgical fields: Comparison of cyberknife multi-sites in Korea. Progress in Nuclear Science and Technology 2011;1:537-40.
12. Dieterich S, Sherouse GW. Experimental comparison of seven commercial dosimetry diodes for measurement of stereotactic radiosurgery cone factors. Med Phys 2011;38:4166-73.
13. Morin J, Beliveau-Nadeau D, Chung E, Seuntjens J, Theriault D, Archambault L, *et al.* A comparative study of small field total scatter factors and dose profiles using plastic scintillation detectors and other stereotactic dosimeters: The case of the cyberKnife. Med Phys 2013;40:011719.
14. Bassinet C, Huet C, Derreumaux S, Brunet G, Chéa M, Baumann M, *et al.* Small fields output factors measurements and correction factors determination for several detectors for a CyberKnife® and linear accelerators equipped with microMLC and circular cones. Med Phys 2013;40:071725.
15. Francescon P, Cora S, Cavedon C, Scalchi P, Reccanello S, Colombo F, *et al.* Use of a new type of radiochromic film, a new parallel-plate micro-chamber, MOSFETs, and TLD 800 microcubes in the dosimetry of small beams. Med Phys 1998;25:503-11.
16. Calcina CS, de Oliveira LN, de Almeida CE, de Almeida A. Dosimetric parameters for small field sizes using fricke xylenol gel, thermoluminescent and film dosimeters, and an ionization chamber. Phys Med Biol 2007;52:1431-9.
17. Jursinic PA. Characterization of optically stimulated luminescent dosimeters, OSLDs, for clinical dosimetric measurements. Med Phys 2007;34:4594-604.
18. Schembri V, Heijmen BJ. Optically stimulated luminescence (OSL) of carbon-doped aluminum oxide (Al2O3:C) for film dosimetry in radiotherapy. Med Phys 2007;34:2113-8.
19. Yukihara EG, Yoshimura EM, Lindstrom TD, Ahmad S, Taylor KK, Mardirossian G, *et al.* High-precision dosimetry for radiotherapy using the optically stimulated luminescence technique and thin Al2O3:C dosimeters. Phys Med Biol 2005;50:5619-28.
20. Viamonte A, da Rosa LA, Buckley LA, Cherpak A, Cygler JE. Radiotherapy dosimetry using a commercial OSL system. Med Phys 2008;35:1261-6.
21. Nascimento LF, Vanhavere F, De Deene Y, Verellen D. Medical dosimetry with a RL/OSL prototype: 6 MV photon beams. Phys Med Eur J Med Phys 2014;30:e25-6.
22. Yukihara EG, Stephen W. Optically Stimulated Luminescence: Fundamentals and Applications. New York: Wiley; 2011.
23. Bøtter-Jensen L, Agersnap Larsen N, Markey BG, McKeever SW. Al2O3:C as a sensitive OSL dosemeter for rapid assessment of environmental photon dose rates. Radiat Meas 1997;27:295-8.
24. Jursinic PA, Yahnke CJ. *In vivo* dosimetry with optically stimulated luminescent dosimeters, OSLDs, compared to diodes; the effects of buildup cap thickness and fabrication material. Med Phys 2011;38:5432-40.
25. Mrčela I, Bokulić T, Izewska J, Budanec M, Fröbe A, Kusić Z, *et al.* Optically stimulated luminescence *in vivo* dosimetry for radiotherapy: Physical characterization and clinical measurements in (60) Co beams. Phys Med Biol 2011;56:6065-82.
26. Spasic E, Adam JF. Optically stimulated luminescence for diagnostic and therapeutic low to medium energy X-ray beams experimental dosimetry. Phys Med Eur J Med Phys 2013;29:e42.
27. Bos AJ. High sensitivity thermoluminescence dosimetry. Nucl Instrum Methods Phys Res Sect B 2001;184:3-28.
28. Emmanuele R, Bonanno E, Cavalli N, Girlando A, Gueli AM, Marino C, *et al*. Characterization of OSLD detectors for dosimetric checks on clinical photon beam. Phys Med Eur J Med Phys 2016;32:21.
29. Charles PH, Crowe SB, Kairn T, Kenny J, Lehmann J, Lye J, *et al.* The effect of very small air gaps on small field dosimetry. Phys Med Biol 2012;57:6947-60.
30. Kerns JR, Kry SF, Sahoo N, Followill DS, Ibbott GS. Angular

dependence of the nanoDot OSL dosimeter. Med Phys 2011;38:3955-62.
31. Lye J, Dunn L, Kenny J, Lehmann J, Kron T, Oliver C, *et al.* Remote auditing of radiotherapy facilities using optically stimulated luminescence dosimeters. Med Phys 2014;41:032102.
32. Yusof FH, Ung NM, Wong JH, Jong WL, Ath V, Phua VC, *et al.* On the use of optically stimulated luminescent dosimeter for surface dose measurement during radiotherapy. PLoS One 2015;10:e0128544.
33. Lehmann J, Dunn L, Lye JE, Kenny JW, Alves AD, Cole A, *et al.* Angular dependence of the response of the nanoDot OSLD system for measurements at depth in clinical megavoltage beams. Med Phys 2014;41:061712.
34. Al-Senan RM, Hatab MR. Characteristics of an OSLD in the diagnostic energy range. Med Phys 2011;38:4396-405.
35. Bekerat H, Devic S, DeBlois F, Singh K, Sarfehnia A, Seuntjens J, *et al.* Improving the energy response of external beam therapy (EBT) gafchromicTM dosimetry films at low energies (≤100 keV). Med Phys 2014;41:022101.
36. Avanzo M, Drigo A, Ren Kaiser S, Roggio A, Sartor G, Chiovati P, *et al.* Dose to the skin in helical tomotherapy: Results of *in vivo* measurements with radiochromic films. Phys Med 2013;29:304-11.
37. Sorriaux J, Kacperek A, Rossomme S, Lee JA, Bertrand D, Vynckier S, *et al.* Evaluation of gafchromic® EBT3 films characteristics in therapy photon, electron and proton beams. Phys Med 2013;29:599-606.
38. Yu PK, Butson M, Cheung T. Does mechanical pressure on radiochromic film affect optical absorption and dosimetry? Australas Phys Eng Sci Med 2006;29:285-7.
39. Nelson R HH, Rogers DW. The EGS4 Code System Stanford Linear Accelerator Center Report SLAC-265. Stanford, CA: SLAC; 1985.
40. Rogers DW, Faddegon BA, Ding GX, Ma CM, We J, Mackie TR, *et al.* BEAM: A Monte carlo code to simulate radiotherapy treatment units. Med Phys 1995;22:503-24.
41. Akselrod MS, Kortov VS, Gorelova EA. Preparation and properties of alpha-Al2O3:C. Radiat Prot Dosim 1993;47:159-64.
42. Walters B, Kawrakow I, Rogers DW. DOSXYZnrc User's Manual Technical Report No. PIRS 794 (RevB). Ottawa, Canada: National Research Council of Canada; 2005.
43. Chalkley A, Heyes G. Evaluation of a synthetic single-crystal diamond detector for relative dosimetry measurements on a cyberknife. Br J Radiol 2014;87:20130768.
44. Azangwe G, Grochowska P, Georg D, Izewska J, Hopfgartner J, Lechner W, *et al.* Detector to detector corrections: A comprehensive experimental study of detector specific correction factors for beam output measurements for small radiotherapy beams. Med Phys 2014;41:072103.
45. Ahmed MF, Shrestha N, Schnell E, Ahmad S, Akselrod MS, Yukihara EG, *et al.* Characterization of Al2O3 optically stimulated luminescence films for 2D dosimetry using a 6 MV photon beam. Phys Med Biol 2016;61:7551-70.